EUROPEAN ORGANIZATION FOR NUCLEAR RESEARCH

CERN – AB DEPARTMENT

Werner.Herr@cern.ch

AB-Note-2006-015 (ABP)

Aperture and beam loss during extraction from the SPS and injection into the CNGS beam line.

G. Arduini, B. Goddard, W. Herr, V. Kain, and M. Meddahi,
AB Department, CERN, 1211-Geneva 23

Abstract

Possible losses in the CNGS proton beam line have been studied for 5B the latest configurations of the beam line and extraction setup. In particular a modified extraction point and the proposed correction were included in the simulation. A detailed study of the effect of the finite rise and fall time of the extraction kicker was performed. We have scanned a large parameter set and derived recommendations for the commissioning procedure, in particular we give the expected loss locations, tolerances on the necessary trajectory correction, performance of the beam position measurement system and beam steering.

Geneva, Switzerland

22 February 2006

1 CNGS proton beam line

1.1 General layout

After the extraction from the SPS, the proton beam is transfered to the target through the proton beam line TT41 [1]. The general CNGS layout is shown in Fig. 1. The proton beam is extracted from the SPS

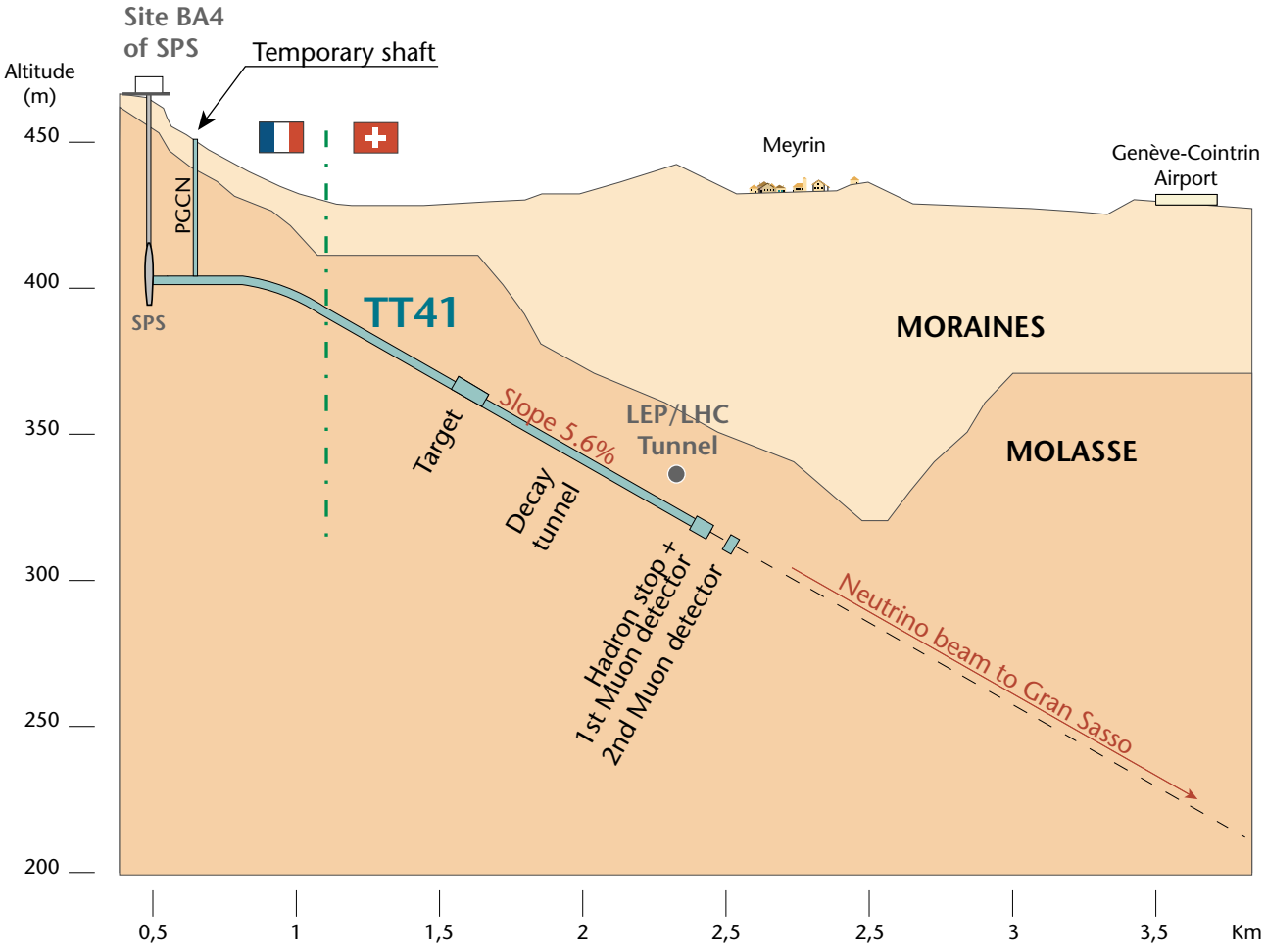

Figure 1: *Overview of the CNGS Layout.*

in LSS4 at 400 GeV, in two consecutive 10.5 μs fast extractions, spaced by 50 ms, in a 6 s cycle. The nominal intensity per extraction is 2.4 10^{13} p/extraction with an upgrade phase to 3.5 10^{13} p/extraction. The CNGS proton beam will be using the same fast extraction channel as the LHC beam in LSS4, and both beams are finally injected into a common beam line (TT40) of about 200 m. At its end the LHC beams are deflected into the transfer line TI8 and the CNGS protons are transferred into the line TT41.

2 Setting up of particle tracking

2.1 Parameters for tracking

For the particle tracking we have used two separate beam lines: a short sequence to describe the SPS extraction up to the start of the transfer line TT40 and another sequence from this injection point to the target point. The optics for the beam line is the version from February 2005. This optics features unequal β-functions at the target to account for unequal emittances of the beam from the SPS. We have therefore β_x^* = 10 m and β_y^* = 20 m at the target. For the normalized emittances of the extracted beam we use ϵ_x^* = 12 μm and ϵ_y^* = 10 μm, respectively (slightly larger than foreseen).

In order to probe particles at large amplitudes, we have not simulated a multi particle beam with a Gaussian amplitude distribution, but rather have tracked particles with fixed amplitudes. The results can then be convolved with the transverse distribution function expected for the beam. This procedure is fully justified since a Gaussian distribution of the tails is highly unlikely.

2.2 Transverse offset correction

At the start of the proton beam line TT40 the extracted beam is offset by approximately 2 mm in the horizontal plane. This is due to the arrangement of the extraction channel to be able to accept LHC and CNGS beams without physical displacement of the extraction septum. The derived settings of the extraction elements are slightly different for the two beams. Without any correction this effect would result in a trajectory shown in Fig. 2. This could in principle be corrected with the standard trajectory

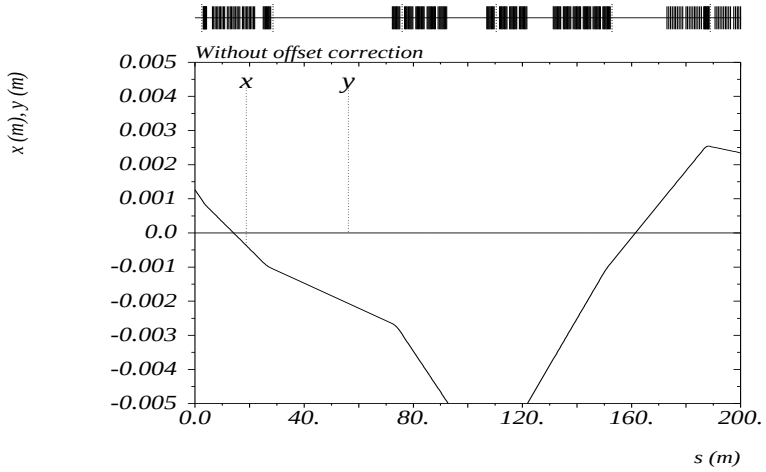

Figure 2: *Injection offset without correction.*

correction procedure. However, this would require rather large strengths in the orbit correctors. To overcome this, the extraction settings have been arranged in both LHC and CNGS cases such that the beam returns to the axis of TT40 at the centre of the first bending family MBHC with zero offset and a finite horizontal angle, allowing the trajectory to be corrected easily with a static adjustment of the MBHC strength. For CNGS a change of the MBHC bending strength of about 6 % is necessary to flatten the trajectory. The result of this procedure is shown in Fig. 3.
To demonstrate the advantage of this manipulation, we show in Fig. 4 the distribution of required strengths of horizontal orbit correctors, which have been computed to correct the trajectory of the line for a large sample of orbit errors. The tail in the distribution of the required strength is due to the correction of the offset which has disappeared in the corrected case.

2.3 Trajectory correction

The trajectory distortion from displaced quadrupoles can be corrected with a static correction as demonstrated in a previous report [2].

2.3.1 Correction strategy

The standard procedures implemented in the MAD-X [5] program have been used, using the theoretical optics.

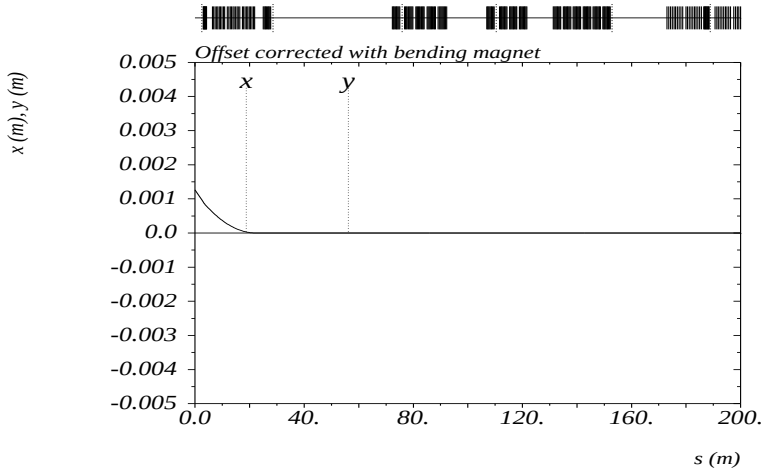

Figure 3: *Injection offset with correction.*

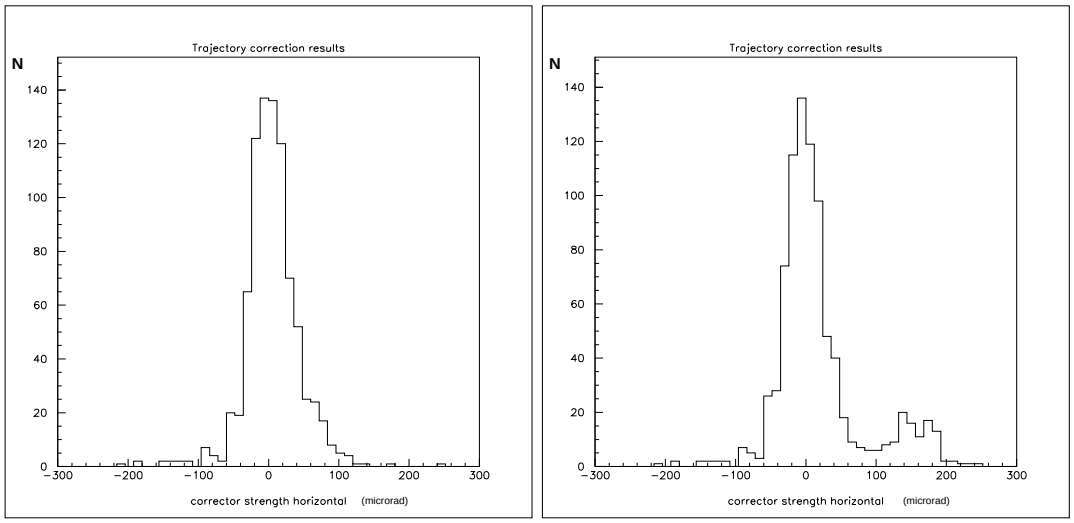

Figure 4: *Necessary strength of horizontal orbit correctors with and without offset correction.*

2.3.2 Quality of correction

Following the implementation of recommendations made in [2], the correction of the trajectory poses no problems for both planes. For the simulation we have defined a minimum correction quality before a particle tracking was performed. The tracking was done separately for maximum orbit distortions of $\pm$ 3 mm, $\pm$ 4 mm and $\pm$ 5 mm to study the dependence on the trajectory after correction.

2.3.3 Incomplete trajectory measurement

To simulate incomplete or faulty trajectory measurements, we have used the MAD-X features [4] to simulate realistic scenarios. In particular, a percentage of missing or faulty beam position monitors can be simulated and the effect on the quality of the orbit or trajectory correction can be evaluated. The consequences of missing measurements are mainly:

- Large trajectory excursions.
- Undetectable distortions.

Both are very undesirable since they affect the steering of the beam on the target or can lead to beam losses at a mechanical aperture limit.

To assess these problems, we have randomly disabled 10 % or 20 % of the monitors before the trajectory correction.

2.4 Fluctuations of injection point

In addition to static trajectory distortions, mainly caused by displaced quadrupoles, the extraction point, i.e. the injection or starting point of TT40/41, may vary from one extraction to the next. As a baseline we have used a displacement of about 0.2 mm (r.m.s.) and an error of the injection angle of 50 μrad (r.m.s.) [2].

2.5 Orthogonal steering

To steer the beam exactly onto the target, 2 orbit correctors (MDS) in each plane are available near the end of the beam line. For this simulation, such a static steering was done for each orbit seed after the trajectory was corrected. Fluctuations, e.g. of the injection, lead to a small deviation of the beam at the target position.
The tracking was done with and without this target steering since we expected that the loss pattern along the beam line might change.

2.5.1 Major aperture limits

The apertures of the beam line elements are implemented using the MAD-X aperture definition [5].

3 Losses in extraction channel

3.1 Extraction trajectory in SPS

The beam is extracted from the SPS with an assembly of a orbit bump, fast kicker magnets (MKE) and separated from the circulating beam with a septum (MSE). The septum is protected by a diluter block (TPSG).

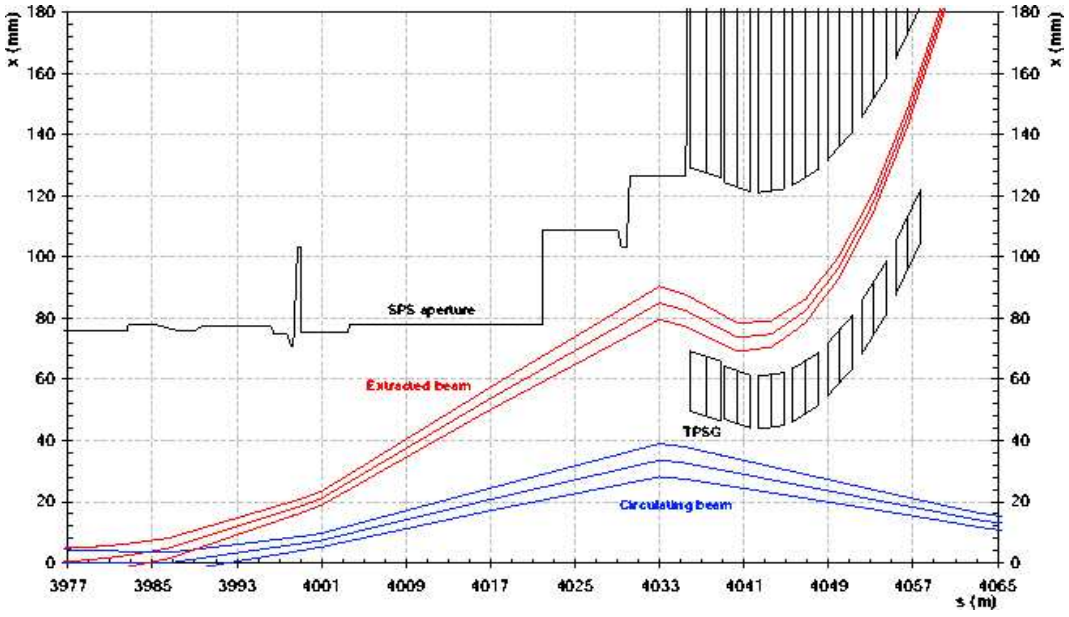

Figure 5: *Extraction channel of the SPS.*

3.2 Nominal extraction trajectory

For the nominal extraction trajectory, the extracted beam is separated by about 0.25 m from the circulating beam using the exit of the SPS quadrupole QD419 as a reference position. This defines the starting point of the transfer line TT40.

3.3 Shape of extraction kicker pulse and beam intensity

The extraction kickers MKE have a finite rise time of about 1 μs. Since during this time the beam cannot be extracted on the foreseen trajectory, a gap is required in the SPS bunch train since otherwise the bunches can be lost in the extraction channel. The shape of this kicker strength (in units relative

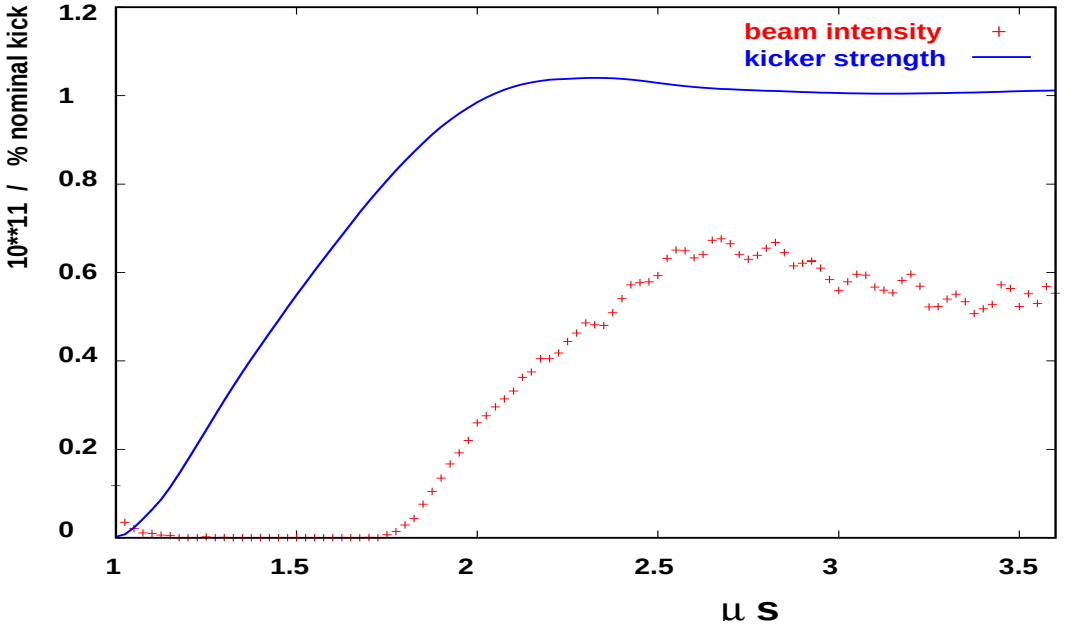

Figure 6: *Extraction kicker shape and intensity in extraction gap. A pedestal of 10^8 particles per bunch is subtracted.*

to nominal strength) and the measured beam intensity in the SPS during the ramp are shown in Fig.6. From this figure we also observe that the ring is populated with bunches before the kickers reach their full strengths. We should therefore like to answer the following questions:

- How does the extraction point move during the kicker rise time ?
- What happens to bunches in the SPS before the kickers have their full strengths ?
- What happens to parasitic bunches in the gap ?

3.3.1 Losses at extraction during kicker sweep

In order to study possible losses during the rise of the kicker strength, particles have been tracked through the extraction channel and subjected to different strengths of the MKE kickers. We have considered particles up to 7 σ of the nominal beam size. It was found that particles inside a 7 σ contour can pass through the entire extraction channel when the kicker strength is above 0.80 (t_{80} = 1.750 μs) of the nominal strength.
Below 0.35 (t_{35} = 1.325 μs) of the nominal strength, particles either stay inside the SPS chamber or they are caught by the TPSG collimator. The corresponding trajectories for the limiting cases and the nominal trajectory are shown in Fig. 7, together with a schematic view of the TPSG.
Inside the window of 0.35 to 0.80 of the nominal strength, part of the beam can pass through and reaches

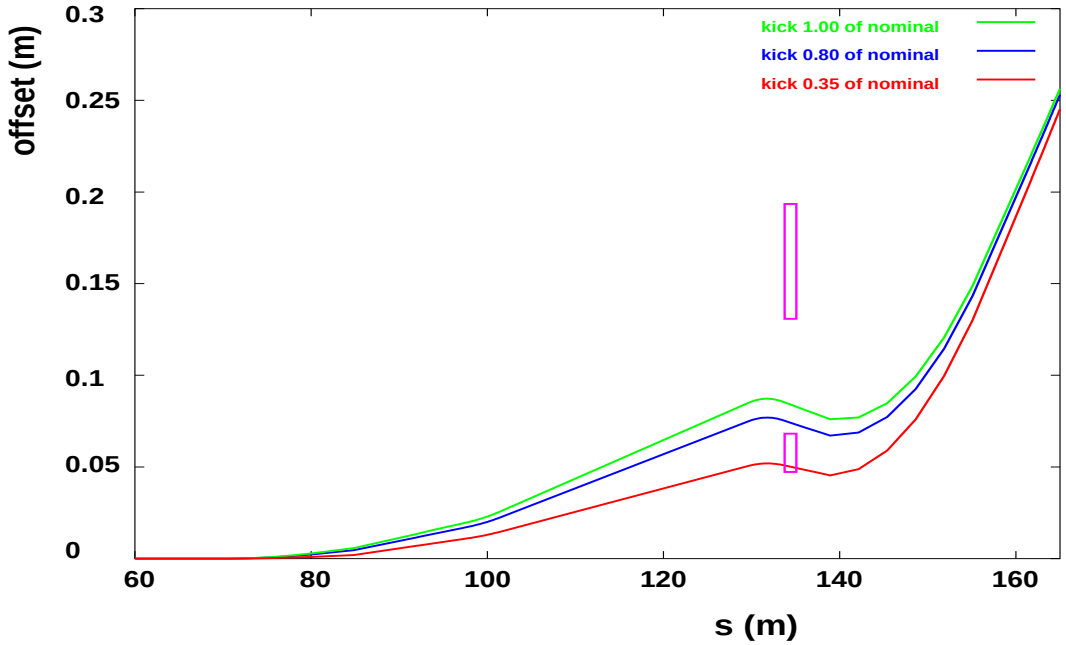

Figure 7: *Extraction trajectories for nominal, 0.80 and 0.35 of nominal kick strength.*

the starting point of TT40. Since these particle are mainly large amplitude particles, their weight to the total beam loss is very small.

This window is shown in Fig. 8. The intensity in a logarithmic scale together with this window is shown

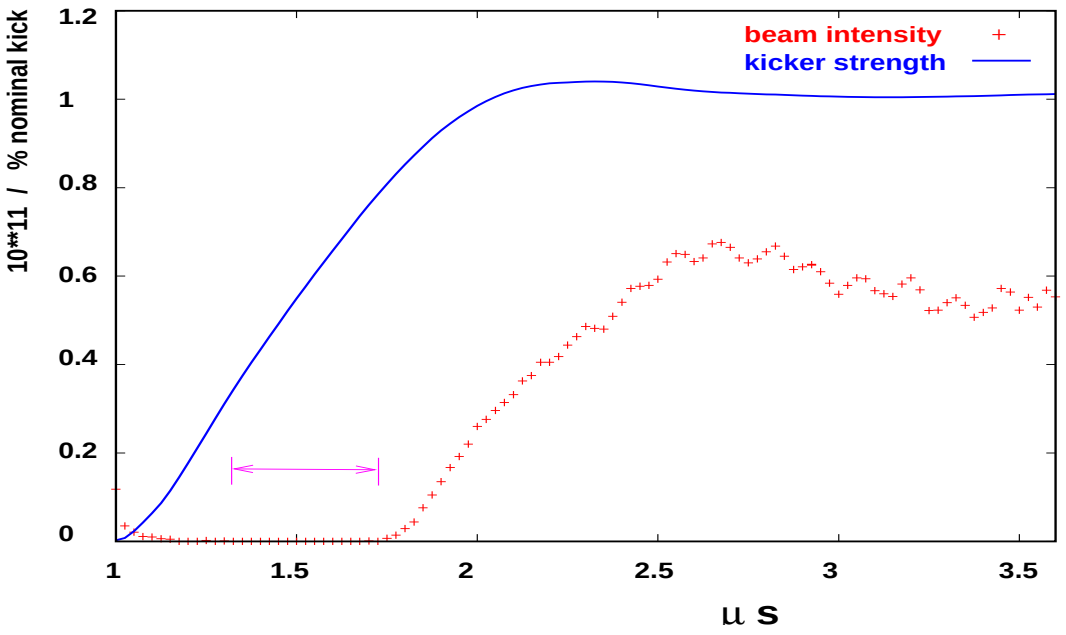

Figure 8: *Extraction kicker shape and intensity in extraction gap. Indicated is the time window where particles can reach TT40/41.*

again in Fig. 9. From Fig. 9 we can derive that we do not expect the corresponding time window to be populated by a significant beam intensity. However, parasitic bunches in the extraction gap would lead to important losses in the extraction channel and, inside the window defined above a significant number of particles arrive at the starting point with largely wrong position and angles. The corresponding shape of the kicker strength and the beam intensity for the falling part is shown in Fig. 10.

From this figure we can draw similar conclusions: from the intensity measurements we do not expect

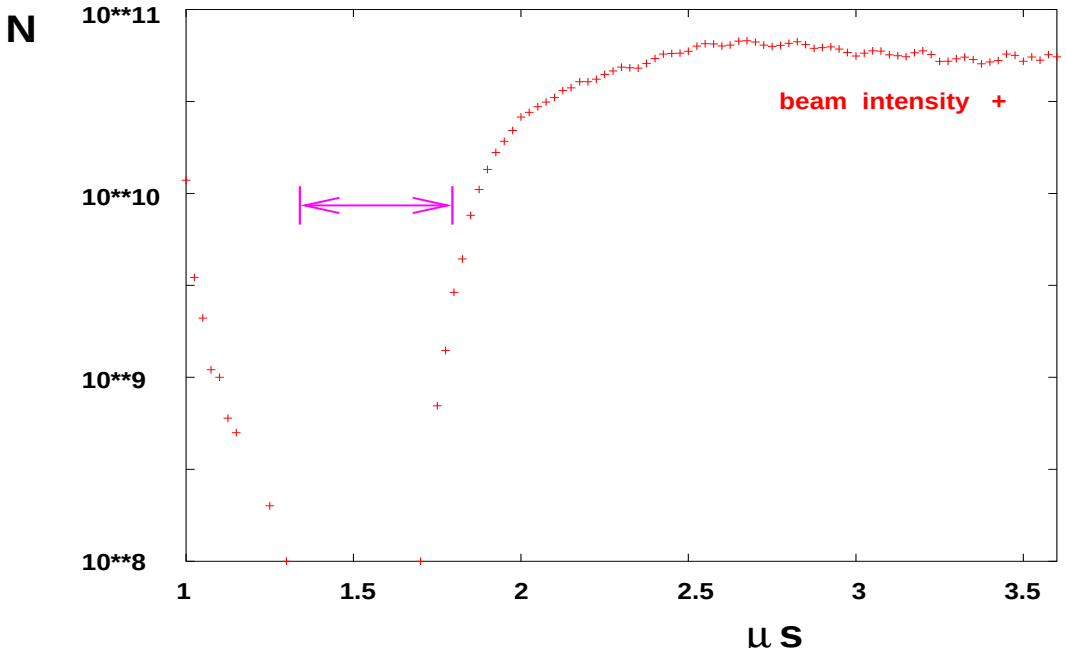

Figure 9: *Intensity in extraction gap in logarithmic scale. Indicated is the time window where particles can reach TT40/41.*

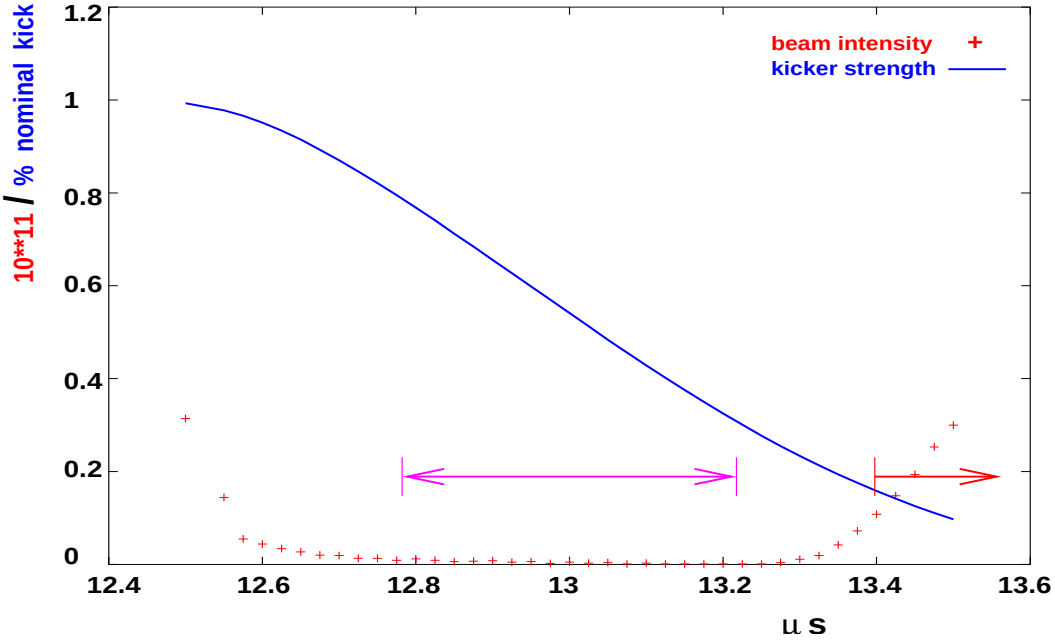

Figure 10: *End of extraction kicker shape and intensity in extraction gap.*

particles to reach TT40 and TT41. Significant intensity is measured at the end of the fall (see Fig.10) and the particles are lost on the TPSG or stay in the SPS. Above the kicker time of 13.4 μs (see Fig.10) a 4 σ beam stays in the SPS. Assuming again a Gaussian beam profile and integrating the bunch positions, not more than 1 to 2 $\cdot$ 10^{10} particles hit the TPSG. Integrating over all bunches from Fig.10 the total loss amounts to $\approx$ 1.2 $\cdot$ 10^{11} particles, where the largest fraction stays inside the SPS.

4 Losses in TT40 and TT41

4.1 Criteria for beam losses

A particle is considered lost in the beam line when its amplitude exceeds the aperture of a beam line element in at least one plane. The amplitude and position of every lost particle are recorded for post-processing.

4.2 Beam losses caused by injection fluctuations and imperfections

4.2.1 Injection errors

We have first studied the effect of injection errors and determined the maximum particle amplitude without losses. A random displacement of all quadrupoles with r.m.s. of 1 mm was simulated and

injection errors (mm/μrad)	max amplitude without loss (units of σ)
0.2/50	$8.4 \pm 0.5\ \sigma$
0.4/100	$7.0 \pm 0.5\ \sigma$
0.6/150	$6.0 \pm 0.4\ \sigma$
0.8/200	$4.5 \pm 0.3\ \sigma$

Table 1: *Effect of injection errors: maximum amplitudes without loss.*

corrected, assuming a fully operational monitoring and correction system.
The results are summarized in Tab. 1. For the (already pessimistic) assumption of injection fluctuations of up to 0.4 mm r.m.s. position errors and 100 μrad r.m.s. angle errors, we do not expect severe particle losses under the described conditions.

4.2.2 Effect of trajectory errors and correction

In a realistic environment, the orbit cannot be corrected below a certain quality. In Tab.2 we show which fraction of particles at 9 σ amplitude are lost in the beam line for different requirements on the quality of the orbit correction. All monitors are assumed working in this case, i.e. no undetectable distortions (bumps) are present. Under these conditions the losses are small, even for badly corrected trajectories. However, the results suggest that one should aim at maximum orbit distortions of about $\pm$ 3 mm.

4.2.3 Effect of missing monitors and orthogonal steering

This pictures changes quickly when we allow for missing or faulty monitors. For the results shown in Tab. 3 we have repeated the previous exercise. Assuming 10 % or the monitors not working, trajectories with peak orbit of $\pm$ 4 mm show already significant losses. Most of the particles are lost on the collimators in front of the target. A very substantial improvement we get when the beams are steered onto the target with the foreseen orbit correctors (3rd column in Tab. 3).
This orthogonal steering onto the target threads the beam through the diluter and reduces the beam losses very significantly up to rather badly corrected orbits.

maximum orbit distortion (mm)	loss of particles at 9 σ amplitude (percentage lost)
$\pm$ 3	0.3 $\pm$ 0.2 %
$\pm$ 4	3.5 $\pm$ 0.5 %
$\pm$ 5	3.9 $\pm$ 0.5 %
$\pm$ 8	5.2 $\pm$ 0.5 %

Table 2: *Effect of trajectory correction quality. All monitors working, r.m.s. injection errors (0.4 mm, 100 μrad).*

maximum orbit distortion (mm)	loss (9 σ), no steering (percentage lost)	loss (9 σ), steering to target (percentage lost)
$\pm$ 3	0.3 $\pm$ 0.2 %	0.3 $\pm$ 0.1 %
$\pm$ 4	8.3 $\pm$ 0.5 %	0.3 $\pm$ 0.1 %
$\pm$ 5	9.1 $\pm$ 0.5 %	0.4 $\pm$ 0.1 %
$\pm$ 8	11.3 $\pm$ 0.5 %	2.1 $\pm$ 0.3 %

Table 3: *Effect of trajectory correction quality. Only 90 % of monitors working, r.m.s. injection errors (0.4 mm, 100 μrad).*

4.3 Effect of extraction kicker sweep

It was shown earlier that a fraction of the beam can reach the start of the CNGS beam line even when the extraction kickers have not reached the nominal values. In particular this is true for parasitic bunches in the extraction gap of the SPS bunch train. For these particles the initial conditions at the beginning of the transfer lines are different from nominal and they might be lost along the trajectory. Since these are caused by a dynamic effect, they cannot be corrected with orbit correctors and add a systematic and time dependent offset to the injection point.

4.3.1 Extraction point during kicker sweep

As a consequence of this dynamic effect, the end point of the trajectories in the extraction channel, i.e. the starting point for the beam line moves during the kicker ramp. This is shown in Fig. 11, where the starting position is plotted versus starting angle. The begin of the kicker rise is the upper left end of the line and the end is the lower right end point.
The position moves by about 15 mm and the angle changes by 1.5 mrad. The acceptance of the beam line TT40 is smaller than that and therefore beam can pass through the line only for a certain window.

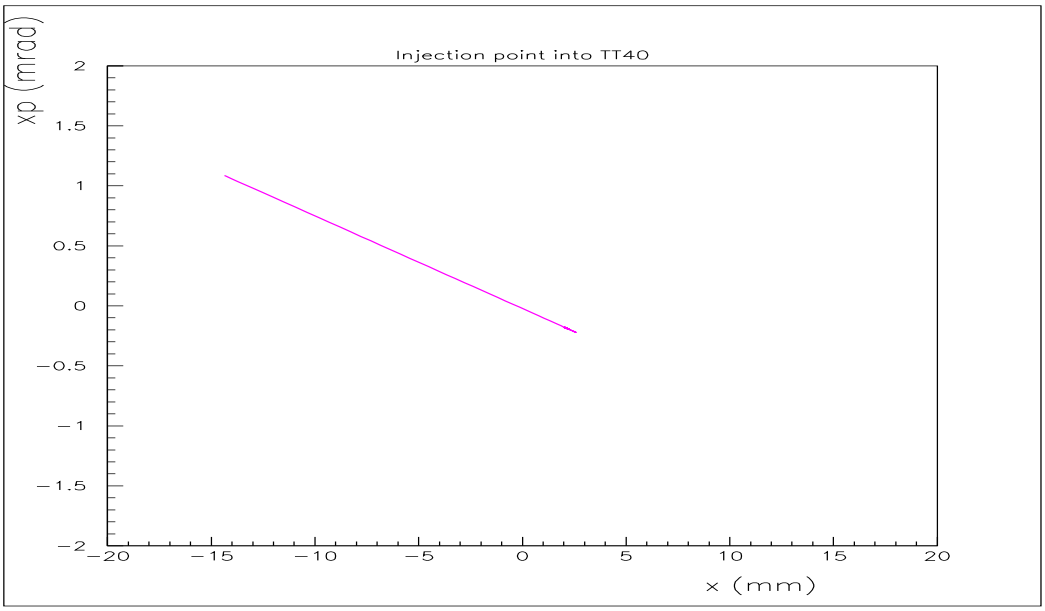

Figure 11: *Theoretical starting point in TT40 along the full kicker sweep. Start of rise upper left, end is lower right.*

4.3.2 Particle losses during kicker sweep

To simulate the particle losses we have used the same procedure as before, assuming a trajectory with $\pm$ 4 mm excursion and beam steering onto the target. For the simulation we used particles up to 9 σ, and adjusted the starting point according to the kicker timing (Fig. 11). The relative loss of particles for

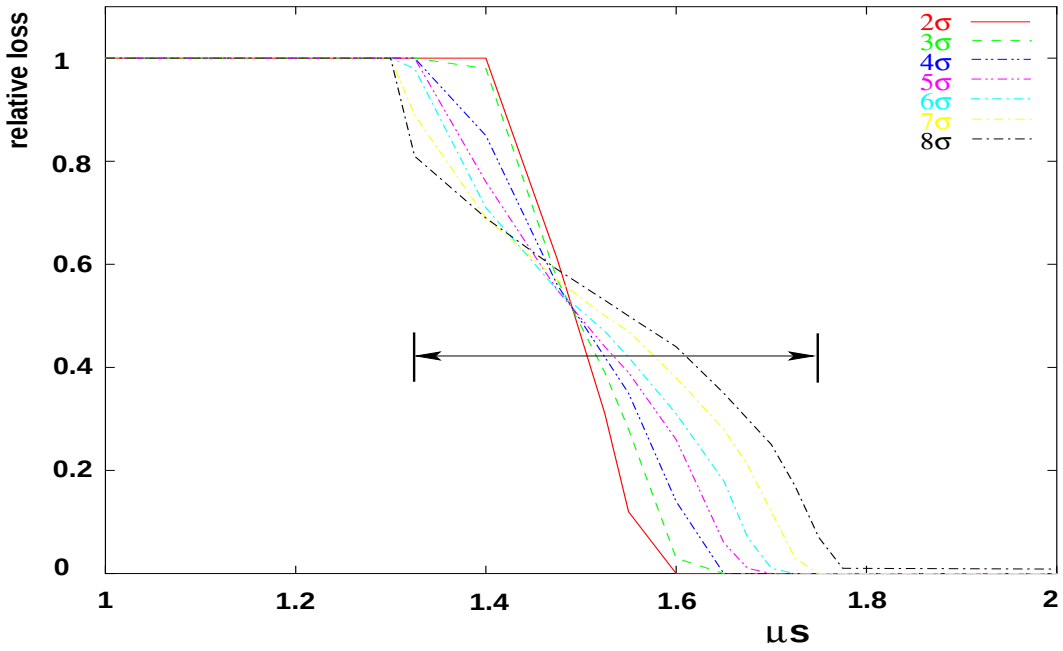

Figure 12: *Relative particle loss in TT40/41 for several amplitudes as function of kicker time.*

amplitudes between 2 σ and 8 σ is shown in Fig. 12 as a function of the kicker timing. Indicated is the timing range where a fraction of the beam can pass through the extraction channel (see Fig. 7).
The increased loss for small amplitudes is due to a large trajectory excursion caused by the ”wrong” horizontal starting point, caused by the kicker sweep. The centre of the beam is moved beyond the

aperture limit.
The losses drop to small values around 1.70 to 1.75 μs, corresponding to about 0.80 of the nominal kick strength. For the large amplitudes above 6 σ in this simulation, folding the distribution with the bunch population in the SPS bunch train gives negligible losses in TT40 and TT41. The orthogonal steering of the beam onto the target is less important since it can only correct for static effects. Assuming a strictly Gaussian distribution, we expect less than 10 particles lost. However, this number can easily be increased by several orders of magnitude when large, non-Gaussian tails are present.

4.4 Parasitic bunches in the extraction gap

Assuming bunches with full intensity in the extraction gap, one must expect losses in both, the extraction channel and TT40/41. Assuming a rather conservative scenario, i.e. substantial fluctuations at injection and trajectory distortions, we have simulated the whole extraction chain along the kicker sweep. While most of the particles are lost at the beginning of the extraction channel, we estimated that in the worst case about 2000 particles are lost in TT40/41 from a bunch with an intensity of 10^{11} protons. These largest losses occur in a window between 1.5 and 1.7 μs (Fig.12). The longitudinal loss pattern is discussed in the next section. Again it shows the importance to have a clean extraction gap.
Under the assumption that **all** bunch positions in the gap are filled with bunches with a maximum intensity of 10^8 protons, we can estimated a total of 20 to 30 protons lost from the beam in TT40/41 using Gaussian tails for the beam profile.

4.5 Position of losses

An important issue is the loss pattern, i.e. the longitudinal position where the particles are lost. In case of parasitic bunches in the extraction gap, we have studied the possible loss pattern for different values of the kicker timing. Particles were tracked through the extraction channel and TT40/41 and the

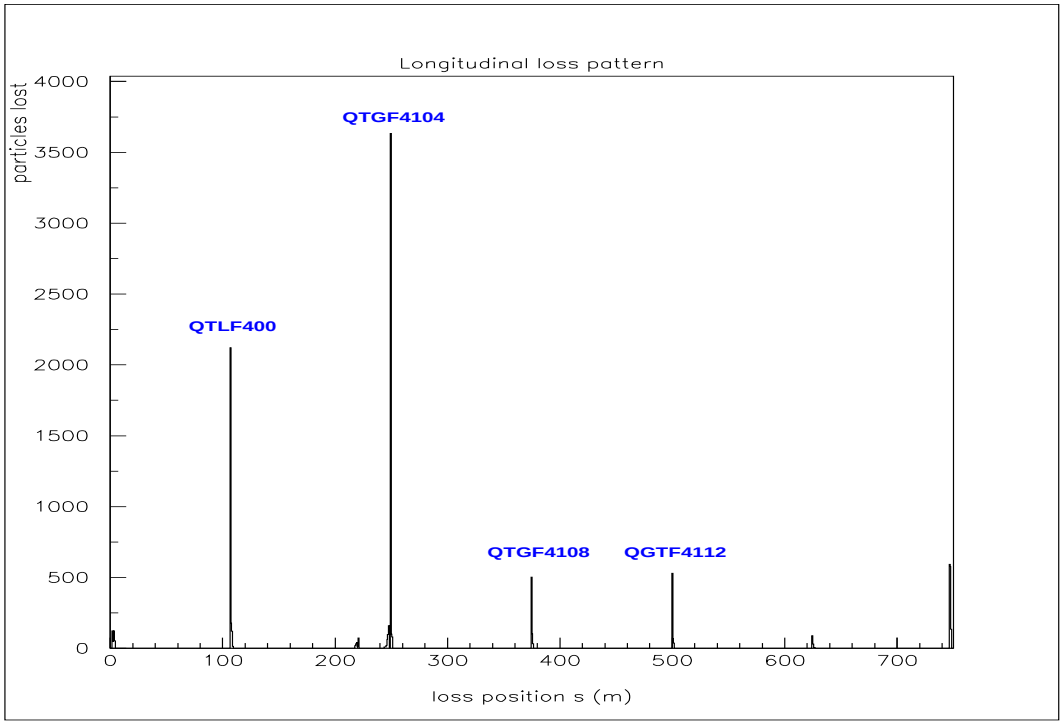

Figure 13: *Loss pattern for 6 σ particles at 0.35 (t_{35} = 1.325 μs) of nominal kick strength.*

longitudinal positions of the losses were recorded. The results are shown in Figs. 13 to 15 corresponding to 0.35, 0.65 and 0.75 of the nominal kick strength.
The results are interesting as well as they are important: while for a kicker strength close to the nominal

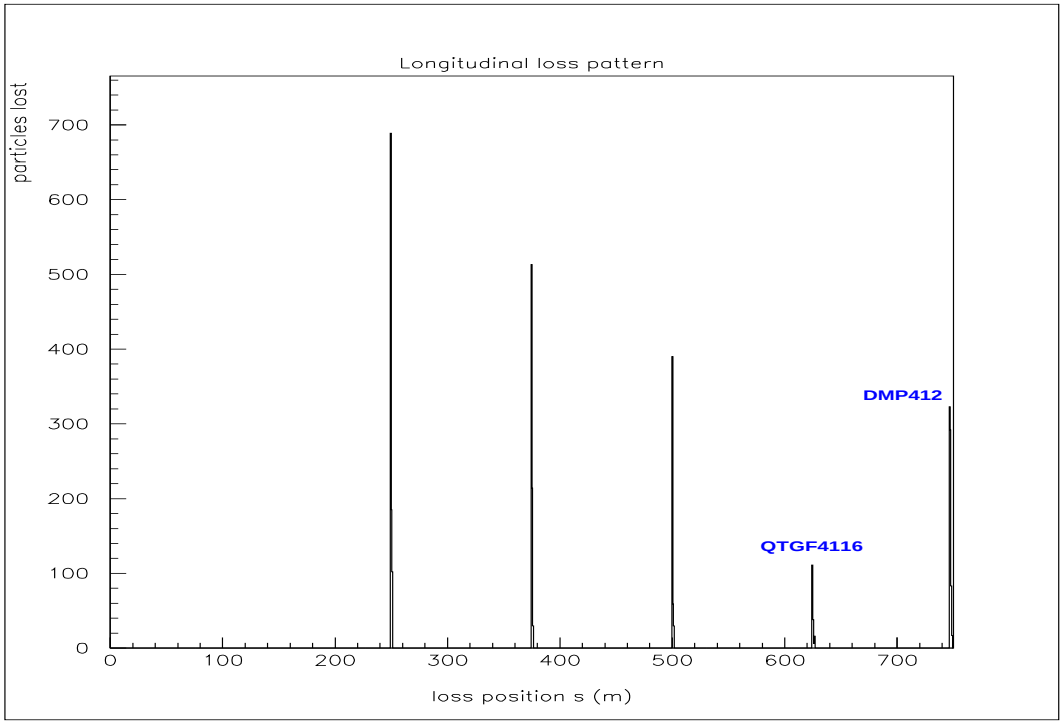

Figure 14: *Loss pattern for 6 σ particles at 0.65 (t_{65} = 1.600 μs) of nominal kick strength.*

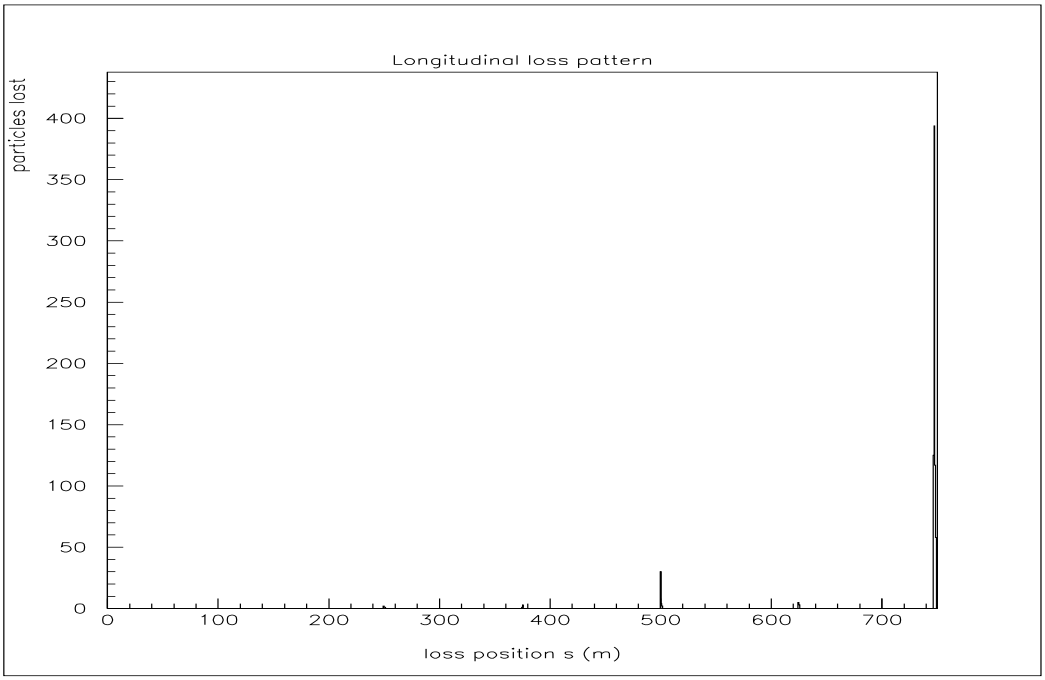

Figure 15: *Loss pattern for 6 σ particles at 0.75 (t_{75} = 1.700 μs) of nominal kick strength.*

value the losses are merely at the end of the beam line and close to the collimators, for bunches early at the kicker ramp the losses occur at the beginning of the line, mainly at the quadrupole QTGF4104 at around 250 m from the start. Only parasitic bunches in the extraction gap fall into this category. Particles with larger amplitude show the identical pattern.

5 Conclusions

We have studied possible beam losses in the extraction channel and TT40/TT41 using a simulation program and realistic (but rather pessimistic) assumptions for imperfections and the correction possibilities.
We conclude with the following recommendations:

- Injection fluctuations are important for beam losses and should be kept small (below 0.2 mm position and 50 μrad angular fluctuations).
- The orbit should be corrected to distortions better than $\pm$ 3 mm.
- Orthogonal steering on the target reduces losses at the end of the line and is mandatory.
- The finite kicker rise time can lead to losses in both, the extraction channel and TT40/TT41 for large amplitude particles inside a acceptance time window of the kicker timing.
- Parasitic bunches in the extraction gap are a problem and must be avoided.
- Under nominal conditions no significant losses should be expected.

References

[1] K. Elsener, editor; *The CERN neutrino beam to Gran Sasso*, Conceptual Technical Design, CERN 98-02, INFN/AE-98/05, 19 May 1998. LHC Project Report 719 (2004).

[2] W. Herr and M. Meddahi; *Trajectory Correction studies for the CNGS proton beam line*, SL-Note-2002-015 AP, May 2002.

[3] W. Herr and M. Meddahi; *Aperture and stability studies for the CNGS proton beam line TT41*, SL-Note-2003-020 AP, March 2003.

[4] W. Herr; *Implementation of new orbit correction procedures in the MAD-X program*, CERN-SL-2002-48 (AP) (2002).

[5] *The MAD-X Home Page, version February 2003*,
http://cern.ch/frank.schmidt/Xdoc/mad-X.html.